

Calibration of a Density-based Model of Urban Morphogenesis

Raimbault Juste^{1,2,*}

1 UMR CNRS 8504 Géographie-cités, Paris, France

2 UMR-T 9403 IFSTTAR LVMT, Champs-sur-Marne, France

*** Corresponding Author**

Email : juste.raimbault@polytechnique.edu

Abstract

We propose a stochastic model of urban growth that generates spatial distributions of population densities, at an intermediate scale between economic models at the macro scale and land-use evolution models focusing on local relations. Integrating simply the two opposite key processes of aggregation (“preferential attachment”) and diffusion (urban sprawl), we show that we can capture the whole spectrum of existing urban forms in Europe. An extensive exploration and calibration of the proposed model allows determining the region of parameter space corresponding morphologically to observed european urban systems, providing an validated thematic interpretation to model parameters, and furthermore determining the effective dimension of the urban system at this scale regarding morphological objectives.

Introduction

Urban Systems are complex socio-technical systems which can be studied from a large variety of viewpoints and disciplines: Batty has advocated in that sense for the construction of a dedicated science defined by its objects of study more than the methods used [1]. Simulating urban growth is one typical aspect As the short term trend is towards a mostly urbanized

[2] propose a micro-based model of urban growth, with the purpose to replace non-interpretable physical mechanisms with agent mechanisms, including interactions forces and mobility choices. Local correlations are used in [3], which develops the model introduced in [4], to modulate growth patterns to resemble real configurations.

[5] morphogenesis for roads

Cellular automata [6]

[7]

In the same spirit, our model situates at similar scales and can be qualified as a morphogenesis model.

The rest of this paper is organized as follows: we first describe formally the model and the morphological indicators; we then develop results of real morphological measures, model exploration and model calibration.

Material and Methods

Urban growth model

Rationale [8] : how Simon model generates power law (paper more general to be quoted ?) ; first mover : path dependency of obtained shapes.

Our model is based on widely accepted ideas of diffusion-aggregation processes for Urban Processes. The combination of attraction forces with repulsion, due for example to congestion, already yield a complex outcome that has been shown under some simplifying assumptions to be representative of urban growth processes. Such a model is studied by [9]. Indeed, the tension between antagonist aggregation and sprawl mechanisms may be an important process in urban morphogenesis. For example [10] opposes centrifugal forces with centripetal forces in the equilibrium view of urban spatial systems, what is easily transferable to non-equilibrium systems in the framework of self-organized complexity : a urban structure is a far-from-equilibrium system that has been driven to this point by these opposite forces. The two contradictory processes of urban concentration and urban sprawl are captured by the model, what allows to reproduce with a good precision a large number of existing morphologies.

The question at which scale is it possible and relevant to define and try to simulate

urban form is rather open, and will in fact depend on which issues are being tackled.

Formalization We formalize now the model, together with its parameters and their possible interpretations. The simulation model proceeds iteratively the following way. The world is a square grid of width N , in which each cell is characterized by its population $(P_i(t))_{1 \leq i \leq N^2}$. initially empty, is represented . At each time step, until total population reaches a fixed parameter P_m ,

- total population is increased of a fixed number N_G (growth rate), following a preferential attachment such that

$$\mathbb{P}[P_i(t+1) = P_i(t) + 1 | P(t+1) = P(t) + 1] = \frac{(P_i(t)/P(t))^\alpha}{\sum (P_i(t)/P(t))^\alpha}$$

- a fraction β of population is diffused to cell neighborhood, this operation being repeated n_d times

Indicators [11] : sort of morphological analysis

As our model is only density-based, we propose to quantify its outputs through spatial morphology, i.e. characteristics of density spatial distribution. We need therefore quantities having a certain level of robustness and invariance. For example, two polycentric cities should be classified as morphologically close whereas a direct comparison of distributions (Earth Mover Distance e.g.) could give a very high distance between configurations depending on center positions. To tackle this issue, we refer to the Urban Morphology Analysis literature which proposes an extensive set of indicators to describe urban form [12]. The number of dimensions can be reduced to obtain a robust description with a few number of independent indicators [13]. For the choice of indicators, we follow the analysis done in [14] where a typology of large european cities is obtained in consistence with qualitative knowledge. Let denote $(P_i)_{1 \leq i \leq N}$ the population of cells, sorted in decreasing order, d_{ij} the distance between cells i, j , and $P = \sum_{i=1}^N P_i$ total population. The indicators are the following :

1. Rank-size slope γ , expressing the degree of hierarchy in the distribution, computed by fitting with Ordinary Least Squares a power law distribution by $\ln P_i/P_0 \sim k - \gamma \cdot \ln i/i_0$.

2. Distribution Entropy

$$\mathcal{E} = \sum_{i=1}^N \frac{P_i}{P} \cdot \ln \frac{P_i}{P} \quad (1)$$

3. Spatial-autocorrelation given by Moran index, with simple spatial weights given

by $w_{ij} = 1/d_{ij}$

$$r = \frac{\sum_{i \neq j} w_{ij} (P_i - \bar{P}) \cdot (P_j - \bar{P})}{\sum_{i \neq j} w_{ij} \sum_i (P_i - \bar{P})^2}$$

4. Mean distance between individuals, which captures population concentration

$$\bar{d} = \sum_{i < j} \frac{P_i P_j}{P^2} \cdot d_{ij}$$

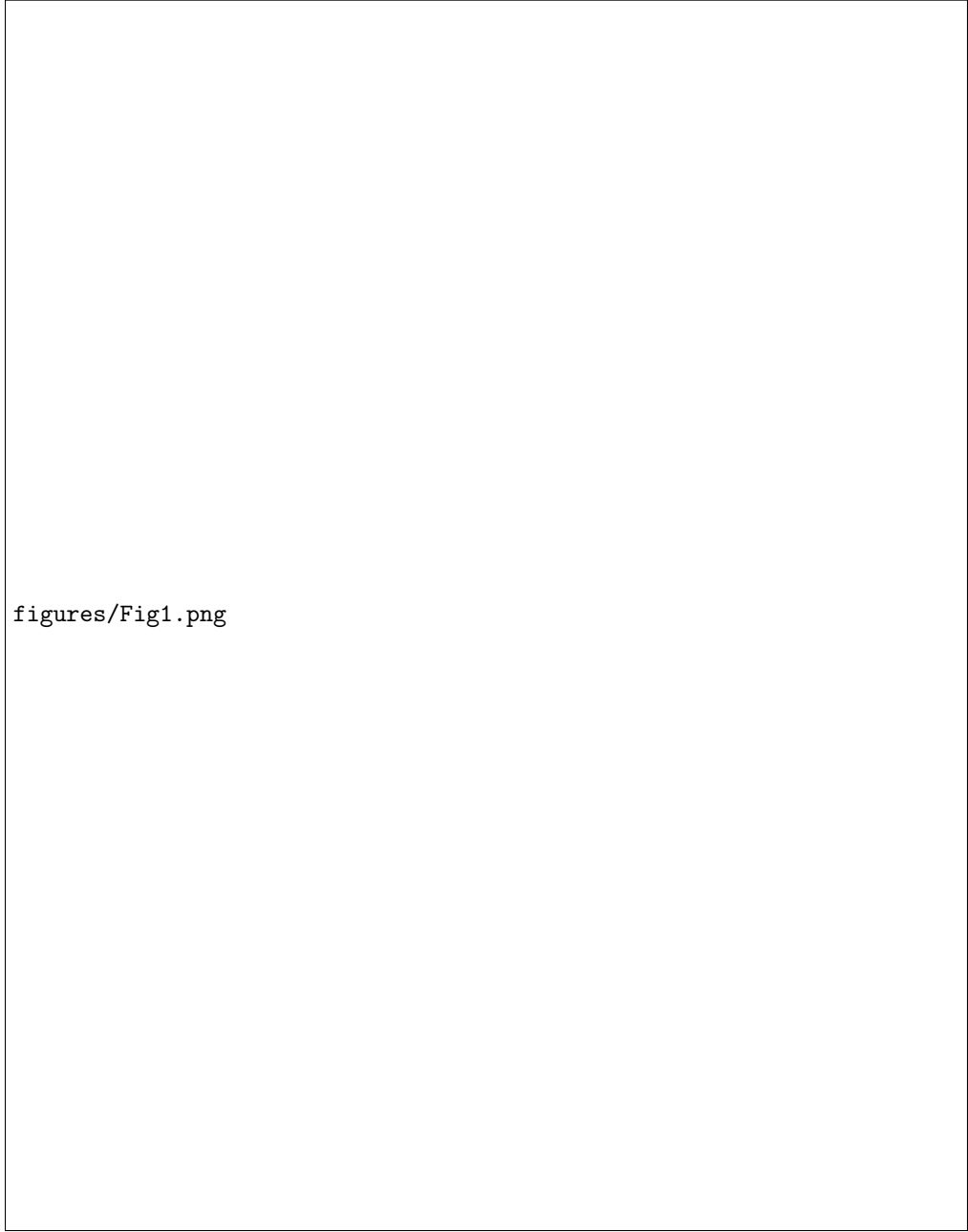
Real Data

We compute morphological measure on real urban density data, namely the population density grid of the European Union at 100m resolution provided openly by Eurostat [15]. The morphological measures used for calibration are the one described above that are the same used to classify model outputs. The calibration of the model is thus done on morphological objectives (entropy, hierarchy, spatial auto-correlation, mean distance). We show in Fig. 1 maps giving values of indicators for France, to ease readability. Maps for the full European union are available in S1 Text. The choice of the resolution, the space range, and the shape of the window on which indicators are computed, is made according to the thematic specifications of the model : We however tested the sensitivity to window size and shape

Results

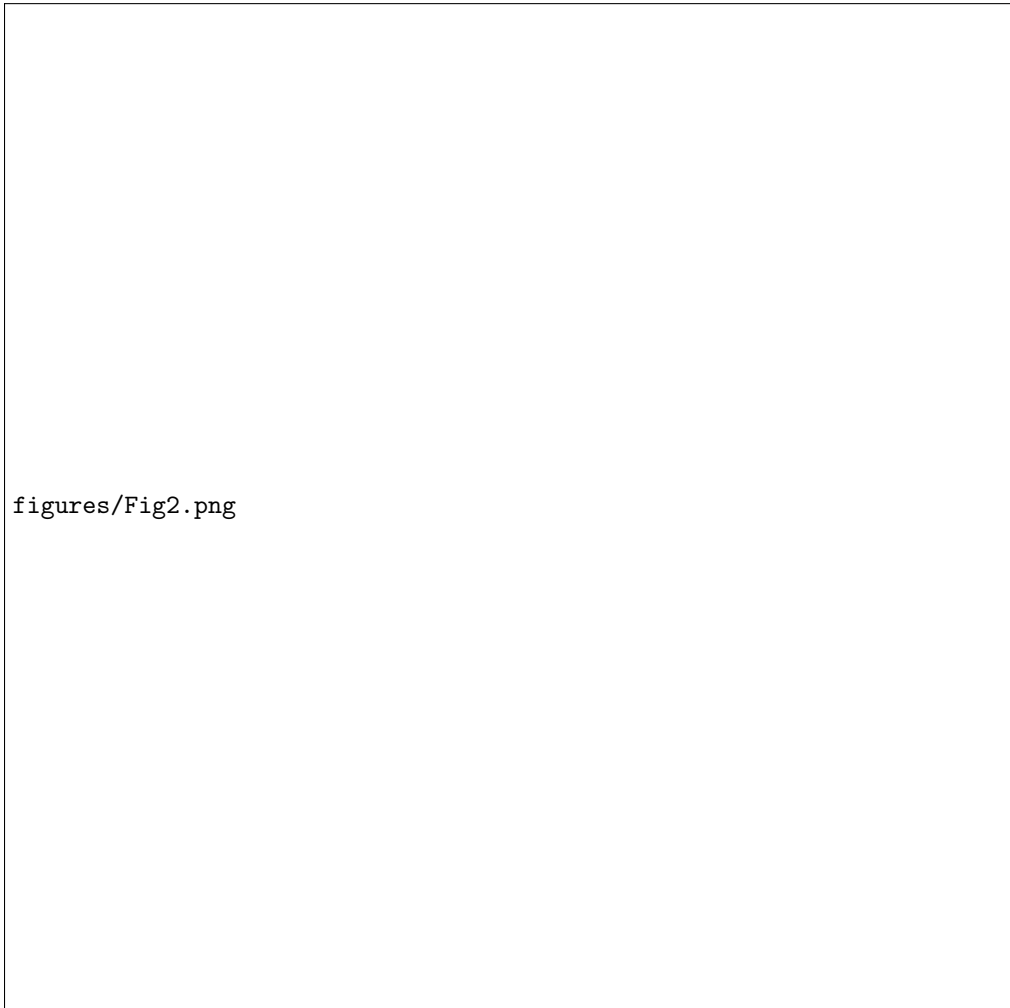
Generation of urban patterns

Implementation The model is implemented both in NetLogo [16] for exploration and visualization purposes, and in **Scala** for performance reasons and easy integration into OpenMole [17], which allows a transparent access to High Performance Computing environments. Computation of indicator values on geographical data is done in **R** using the **raster** package [18]. Source code and results are available on the open repository of the project at <https://github.com/JusteRaimbault/CityNetwork/tree/master/Models/Synthesis>



figures/Fig1.png

Figure 1. Empirical values of morphological indicators.



figures/Fig2.png

Figure 2. Example of the variety of generated urban shapes.

Raw datasets for real indicator values and simulation results are available on Dataverse
at <http://dx.doi.org/10.7910/DVN/WSUSBA>.

Generated Shapes The model has a relatively small number of parameters but is
able to generate a very wide variety of shapes, extending beyond existing forms. In
particular, its dynamical nature allows through P_m parameter to choose final regime that
can be non-stationarity (generally chaotic shapes), semi-stationarity or full stationarity.
Fig. 2 shows examples of generated shapes, and illustrates the variety of forms that can
be produced by the model.

figures/Fig3.png

Figure 3. Behavior of indicators.

Model Behavior

In the study of such a computational model of simulation, the lack of analytical tractability must be balanced by an extensive knowledge of model behavior in the parameter space.

Convergence Indicators show good convergence property and bimodal statistical distribution for cumulated points in the parameter space confirm the existence of superposed regimes : gaussian distribution gives stationary configurations, whereas inverse log-normal distribution are close to real data shape and correspond to non-stationary regime. For one point and a large number of repetitions, we find that 50 repetitions are enough to obtain a 95% confidence interval smaller than σ around indicator mean.

Exploration of parameter space We sample the Parameter space using a Latin Hypercube Sampling. Parameter bounds are $\alpha \in [0.2, 2], \beta \in [0, 0.1], n_d \in \{0, \dots, 4\}, N_G \in [500, 3000], P_m \in [2000, 100000]$.

Semi-analytical Analysis

Our model can be understood as a type of reaction-diffusion model, that have been widely used in other fields such as biology: similar processes were used for example

Figure 4. Calibration of the model. The principal component analysis is conducted to maximize the spread of the differences between real data and model output, i.e. on the set $\{|R_i - M_j|\}$ where R_i is the set of real points, M_j the set of model outputs. We select then the overlapping cloud at threshold θ , by taking models output closer to real point cloud than θ in the (PC1,PC2) plan.

by Turing in its seminal paper on morphogenesis [20]. An other way to formulate the model typical to these approaches is by using Partial Differential Equations. We propose to gain insights into long-time dynamics by studying them on a simplified case. We consider the system in one dimension, such that $x \in [0; 1]$ with $1/\delta x$ cells of size δx . Each cell is characterized by its population as a random variable $P(x, t)$. We work on their expected values $p(x, t) = \mathbb{E}[P(x, t)]$, and assume that $n_d = 1$. As developed in Supplementary Material S2 Text, we show that this simplified process verifies the following PDE:

$$\delta t \cdot \frac{\partial p}{\partial t} = \frac{N_G \cdot p^{\alpha-2}}{P_\alpha(t)} \cdot \left(p^2 + \frac{\alpha \beta \delta x^2}{2} \cdot \left[\frac{\partial^2 p}{\partial x^2} \cdot p + (\alpha - 1) \left(\frac{\partial p}{\partial x} \right)^2 \right] \right) - p \quad (2)$$

We learn the following properties:

1. Existence of a stationary solution for population proportion
2. Characteristic distance of the stationary distribution
3. Existence of bifurcations in the random case

Model Calibration

We use a specific calibration process: a principal component analysis allows to maximize the cumulated distance between generated points and reals points. We select then the point cloud that overlaps real points in the (PC1,PC2) plan, given a distance threshold. Fig. 4 shows the points we obtain for four different values of the threshold ranging from 10^{-6} to 10^{-3} .

Discussion

more refined model : thresholded aggregation and diffusion (distance to center for diffusion, maximum density for aggregation)

figures/Fig5.png

Figure 5. PSE exploration. Scatterplots of Moran against Entropy, with blue points obtained with LHS and red with PSE exploration. Lower bound is in green.

Calibration refinement and Targeted Exploration We plan in further work to extract the exact parameter space covering all real situations and provide interpretation of its shape (correlations between parameters). Its volume in different directions should give the relative importance of parameters.

We also use the parameter space exploration algorithm [19] implemented in Open-Mole, and obtain in Fig. ?? the lower bound in Moran-entropy plan, that unexpectedly exhibit a scaling relationship that we aim to explore further.

Integration into a multi-scale growth model

It could be possible to couple this model with a Gibrat (or Favaro-pumain) at Europa scale (macro) (with addition of consistence on migration constraints), where meso growth rates which were exogenous before are top-down determined, and bottom-up feedback is done through local aggregation level, influence importance of each area.

[21]

Conclusion

144

In conclusion, this first modeling step provide an accurately calibrated spatial urban growth model at the mesoscopic scale that can reproduce any European urban pattern in terms of urban form. Further work is needed for an interpretation of parameter influence and the determination of effective independent dimensions of the urban system at this scale. We will use this model for other purposes in the following.

145

146

147

148

149

Supporting Information

150

S1 Text

151

Extended Model Exploration.

152

S2 Text

153

Semi-analytical Analysis. Analytical and numerical developments of subsection .

154

References

1. Batty M. The new science of cities. Mit Press; 2013.
2. Andersson C, Lindgren K, Rasmussen S, White R. Urban growth simulation from “first principles”. *Physical Review E*. 2002;66(2):026204.
3. Makse HA, Andrade JS, Batty M, Havlin S, Stanley HE, et al. Modeling urban growth patterns with correlated percolation. *Physical Review E*. 1998;58(6):7054.
4. Makse HA, Havlin S, Stanley H. Modelling urban growth. *Nature*. 1995;377(1912):779–782.
5. Courtat T, Gloaguen C, Douady S. Mathematics and morphogenesis of cities: A geometrical approach. *Physical Review E*. 2011;83(3):036106.
6. Ward DP, Murray AT, Phinn SR. A stochastically constrained cellular model of urban growth. *Computers, Environment and Urban Systems*. 2000;24(6):539–558.

7. Frankhauser P. Fractal geometry of urban patterns and their morphogenesis. *Discrete Dynamics in Nature and Society*. 1998;2(2):127–145.
8. Sheridan Dodds P, Rushing Dewhurst D, Hazlehurst FF, Van Oort CM, Mitchell L, Reagan AJ, et al. Simon's fundamental rich-gets-richer model entails a dominant first-mover advantage. *ArXiv e-prints*. 2016 Aug;.
9. Batty M. Hierarchy in cities and city systems. In: *Hierarchy in natural and social sciences*. Springer; 2006. p. 143–168.
10. Fujita M, Thisse JF. Economics of agglomeration. *Journal of the Japanese and international economies*. 1996;10(4):339–378.
11. Guérois M, Pumain D. Built-up encroachment and the urban field: a comparison of forty European cities. *Environment and Planning A*. 2008;40(9):2186–2203.
12. Tsai YH. Quantifying urban form: compactness versus 'sprawl'. *Urban studies*. 2005;42(1):141–161.
13. Schwarz N. Urban form revisited—Selecting indicators for characterising European cities. *Landscape and Urban Planning*. 2010;96(1):29 – 47. Available from: <http://www.sciencedirect.com/science/article/pii/S0169204610000320>.
14. Le Néchet F. De la forme urbaine à la structure métropolitaine: une typologie de la configuration interne des densités pour les principales métropoles européennes de l'Audit Urbain. *Cybergeog: European Journal of Geography*. 2015;.
15. EUROSTAT. Eurostat Geographical Data; 2014. Available from: <http://ec.europa.eu/eurostat/web/gisco/geodata/reference-data/administrative-units-statistical-units>.
16. Wilensky U. NetLogo. 1999;.
17. Reuillon R, Leclaire M, Rey-Coyrehourcq S. OpenMOLE, a workflow engine specifically tailored for the distributed exploration of simulation models. *Future Generation Computer Systems*. 2013;29(8):1981–1990.
18. Hijmans RJ. Geographic data analysis and modeling. 2015;.

19. Chérel G, Cottineau C, Reuillon R. Beyond Corroboration: Strengthening Model Validation by Looking for Unexpected Patterns. PLoS ONE. 2015 09;10(9):e0138212. Available from: <http://dx.doi.org/10.1371/journal.pone.0138212>.
20. Turing AM. The chemical basis of morphogenesis. Philosophical Transactions of the Royal Society of London B: Biological Sciences. 1952;237(641):37–72.
21. Zhang Z, Su S, Xiao R, Jiang D, Wu J. Identifying determinants of urban growth from a multi-scale perspective: A case study of the urban agglomeration around Hangzhou Bay, China. Applied Geography. 2013;45:193–202.